Contents lists available at ScienceDirect

Chemical Engineering Research and Design

journal homepage: www.elsevier.com/locate/cherd

Comparison between three types of ammonia synthesis reactor configurations in terms of cooling methods

*Mohammad Hasan Khademi**, *Reyhaneh Sadat Sabbaghi*

Department of Chemical Engineering, Faculty of Engineering, University of Isfahan, P.O. Box 81746-73441, Isfahan, Iran

ARTICLE INFO

Article history:
Received 27 June 2017
Received in revised form 11 October 2017
Accepted 16 October 2017
Available online 26 October 2017

Keywords:
Ammonia synthesis
Internal direct cooling reactor
Adiabatic quench cooling reactor
Adiabatic indirect cooling reactor
Optimization
Differential evolution

ABSTRACT

In this study, simulation and optimization of ammonia synthesis reactor based on the implemented cooling methods was presented in three cases: internal direct cooling reactor (IDCR), adiabatic quench cooling reactor (AQCR), and adiabatic indirect cooling reactor (AICR). A one-dimensional pseudo-homogeneous model was developed to investigate the effect of various parameters on maximum N_2 conversion at the outlet of IDCR, 2-bed AQCR and 2-bed AICR. Differential evolution algorithm was applied to optimize three types of ammonia synthesis reactor, considering N_2 conversion as the main objective. A comparison between IDCR, 2/3/4-bed AQCR and 2/3/4-bed AICR was carried out under the optimal operating conditions by considering the same catalyst volume, operating pressure and feed mass flow rate for all three types of reactor. The optimization results show that a maximum conversion of 0.26 was achieved in 3-bed AQCR, in which the temperature of feed gas to the first bed was 635 K, dimensionless lengths of each bed were 0.13, 0.25 and 0.62, and fractions of total feed flow rate quenching from the first to end bed were 0.2, 0.26 and 0.54, respectively. The optimum value of N_2 conversion was found 0.3 in IDCR at the gas temperature to the cooling tube of 495 K. In 3-bed AICR, the highest conversion of 0.3 was determined at temperature of inlet gas to each bed, 696 K, and dimensionless length of each bed, 0.33. Generally, IDCR, 3-bed AICR and 3-bed AQCR were suggested as ammonia synthesis reactor configurations from the most favorable to the least favorable.

© 2017 Institution of Chemical Engineers. Published by Elsevier B.V. All rights reserved.

1. Introduction

Ammonia is one of the most useful chemicals in industry. The largest fraction of ammonia is used to produce fertilizers like ammonium nitrate, ammonium phosphate, and urea. Moreover, ammonia is used in the manufacture of explosive materials, fibers, plastics, polymers, papers, and acids. Thus, its synthesis is an important industrial process. The ammonia synthesis reactor is the heart of an ammonia production plant, and design and optimization of such reactor is very important.

The ammonia synthesis reaction is relatively simple, straightforward, and exothermic. The product is stable, and there is no side reaction. The synthesis reaction based on the Haber–Bosch process takes place between gaseous nitrogen (from air) and hydrogen (from steam reforming of methane) at high temperature and pressure over a magnetic iron oxide catalyst with particle size of 6–10 mm.

$$N_2\,(g) + 3H_2\,(g) \leftrightarrow 2NH_3\,(g) + Q \quad (1)$$

Because the reaction is highly exothermic, the ammonia production reactors require a cooling system to achieve a high degree of conversion. Based on the implemented cooling methods, there are three types of ammonia synthesis fixed-bed reactor:

* *Corresponding author.*
E-mail address: m.khademi@eng.ui.ac.ir (M.H. Khademi).
https://doi.org/10.1016/j.cherd.2017.10.021
0263-8762/© 2017 Institution of Chemical Engineers. Published by Elsevier B.V. All rights reserved.

Nomenclature

a_i	Activity of component i
A	Cross section area of bed (m^2)
A_i	Inside surface area of cooling tube per unit length of reactor (m^2/m)
A_o	Outside surface area of cooling tube per unit length of reactor (m^2/m)
$C_{P_{mixf}}$	Specific heat of feed gas mixture (kcal/kmol K)
$C_{P_{mixg}}$	Specific heat of reacting gas mixture (kcal/kmol K)
D_p	Equivalent particle diameter (m)
E	Activation energy (kcal/kmol)
f_i	Fugacity of component i (atm)
$F^0_{N_2}$	Initial molar flow rate of nitrogen (kmol/h)
f_{W_k}	Fraction of total feed flow rate quenching to k^{th} bed
G	Mass velocity in cooling tubes (kg/m^2 h)
G'	Mass velocity in catalyst bed (kg/m^2 h)
h_{io}	Heat transfer coefficient inside cooling tubes (kcal/m^2 h K)
h_o	Heat transfer coefficient inside the bed (kcal/m^2 h K)
h^0_o	Static distribution of h_o (kcal/m^2 h K)
K_a	Equilibrium constant of reaction
K_0	Arrhenius coefficient
k	Reverse reaction rate constant
P	Pressure (atm)
R	Universal gas constant (kcal/kmol K)
R_{NH_3}	Intrinsic rate of reaction (kmol/m^3 h)
Re	Reynolds number
Re'	$= D_pG'/\mu$ Modified Reynolds number
T_f	Temperature of feed gas (K)
T_g	Temperature of reacting gas (K)
T_k	Temperature of inlet gas to k^{th} bed (K)
U	Overall heat transfer coefficient (kcal/h m^2 K)
W	Mass flow rate (kg/h)
X_{N_2}	Nitrogen conversion
y_i	Mole fraction of component i
z	Bed length (m)

Greek letters

η	Effectiveness factor
$\phi_{H_2}, \phi_{N_2}, \phi_{NH_3}$	Fugacity coefficient of hydrogen, nitrogen and ammonia
ξ_k	Dimensionless length of k^{th} bed
ΔH_r	Heat of reaction (kcal/kmol of NH_3)

- Internal direct cooling reactor
- Adiabatic quench cooling reactor
- Adiabatic indirect cooling reactor

1.1. *Internal direct cooling reactor*

In internal direct cooling reactors (IDCR), a cooling medium which flows in most cases in internal tubes of the catalyst bed is used to remove heat. The most important converter type using internal cooling is the Tennessee Valley Authority (TVA) converter. Fig. 1(a) shows a simplified diagram of TVA convertor. In the cooling tubes section, the preheated gas flows upward inside a large number of small tubes; part of the heat generated in the catalyst bed removes by this section. At the top of the reactor the synthesis gas, now brought to a sufficient temperature, reverses its direction and flows downward through the catalyst bed where the ammonia synthesis reaction occurs.

Numerous researches on the mathematical modeling and optimization of ammonia synthesis TVA reactor have been done. Baddour et al. (1965) developed a simple steady-state model for TVA converter to investigate the effect of space velocity, feed gas ammonia and inert contents, reactor heat conductance, and catalyst activity upon reactor stability, ammonia production rate, and catalyst bed temperature profile. Murase et al. (1970) used the maximum principle to optimize converter performance by considering the heat transfer coefficient between the catalyst bed and cooling tubes as a decision variable. Elnashaie et al. (1988b) investigated the effect of various parameters such as heat transfer coefficient, space velocity of feed gas and ammonia concentration on the performance and stability of the reactor. Also, there are many researches that find an optimal reactor length to maximize the economic return subject to a number of coupled differential-algebraic equations as constraints by using different approaches like genetic algorithm (GA) (Upreti and Deb, 1997; Ksasy et al., 2010), nested differential evolution (DE) (Babu et al., 2004), Quasi-Newton (QN) (Babu and Angira, 2005), gravitational search algorithm (GSA) (Borges et al., 2012) and golden search (GS) method (Carvalho et al., 2014).

1.2. *Adiabatic quench cooling reactor*

In adiabatic quench cooling reactors (AQCR), a cooling system is applied by injection of cold, unconverted feed gas between separate catalyst beds. The most important example of this converter type is the M. W. Kellogg 3 or 4-bed quench converter which was used in a large number of plants. A simplified drawing of a 4-bed converter is shown in Fig. 1(b). The reactor inlet gas is divided into four parts: mainstream, first quench flow, second quench flow, and third quench flow. The mainstream of gas passes through the internal heat exchanger to preheat and then enters the first bed. After passing through the first bed, the temperature is increased. The output gas from the first bed is quenched with the first quench flow and consequently its temperature is decreased. At the same time, the ammonia concentration decreases because the exit gas from the first bed is diluted with unconverted gas. After that, it is sent into the second bed. Similarly, the output gas from each bed is mixed with such quench flow and is entered to the next bed.

Gaines (1977) developed a steady-state model for a quench-type ammonia converter and studied the effect of converter temperature profile over a large range of operating conditions. Sadeghi and Kavianiboroujeni (2009) estimated the process behavior of an industrial 4-beds ammonia synthesis reactor using one and two-dimensional models; the reactor performance was optimized by applying the GA in varying quench flows. Shah (1967) carried out a control simulation for ammonia synthesis process to predict the quench-type reactor behavior specially ammonia yield when changes are made in the controllable variables of the reactor. Reddy and Husain (1982) simulated an ammonia synthesis loop containing a quench-type converter to investigate the effects of H_2/N_2 ratio in the recycle gas, loop pressure, recycle gas flow rate, and inert concentration on the ammonia production rate, fractional hydrogen conversion, and gross profitability.

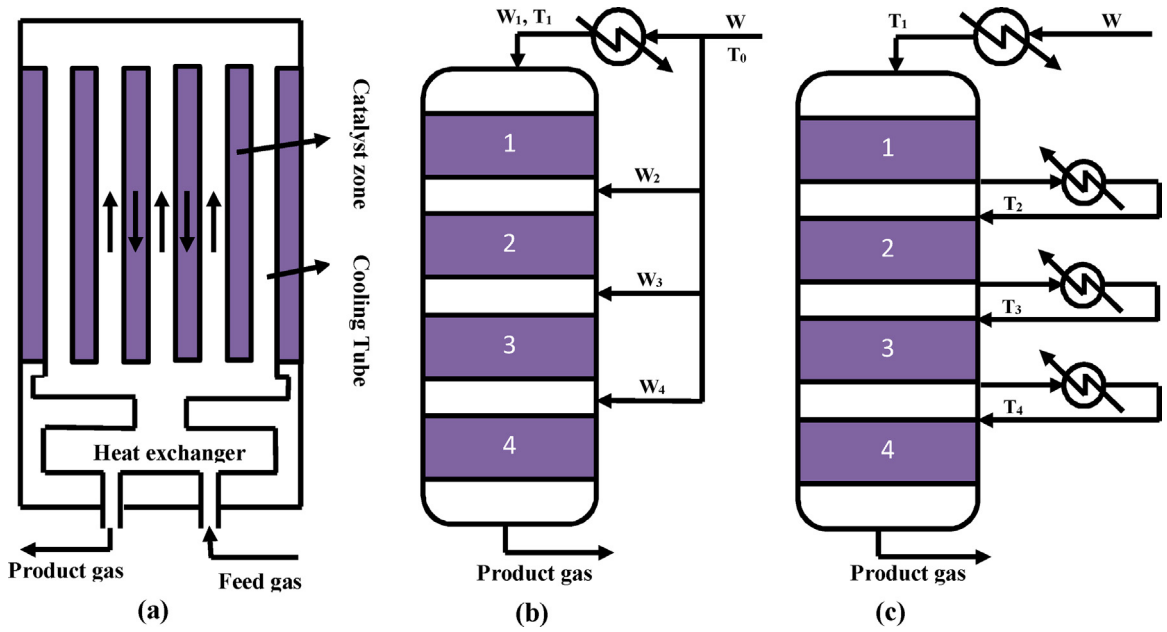

Fig. 1 – A schematic diagram of (a) internal direct cooling reactor, (b) adiabatic quench cooling reactor, and (c) adiabatic indirect cooling reactor.

1.3. *Adiabatic indirect cooling reactor*

In adiabatic indirect cooling reactor (AICR), the cooling required to reach a desired high conversion in the converter is provided between the catalyst beds by some cooling medium, which most often is synthesis gas or boiler feed water. The heat exchange most often takes place in exchangers installed together with the catalyst beds inside one pressure shell, although external heat exchangers installed between separate, adiabatic converters have also been used. In contrast to the AQCR, all gas passes through all catalyst beds, and there is no dilution of the partially converted gas between catalyst beds. A schematic diagram of AICR is shown in Fig. 1(c).

Only a few papers in the literature are concerned with mathematical modeling of AICR. Elnashaie et al. (1988a) and Dashti et al. (2006) used a heterogeneous model to simulate and optimize an industrial reactor having three adiabatic beds with inter stage cooling.

1.4. *Comparison between IDCR, AQCR and AICR*

Recently, two researches have been carried out to compare the behavior of these reactor configurations. Azarhoosh et al. (2014) used a one-dimensional heterogeneous model to investigate the effect of inlet temperature, total feed flow rate and operating pressure on the ammonia production in two cases: first, a horizontal AICR of the Khorasan petrochemical plant, second, a horizontal AQCR with two quench flows. Finally, optimum solutions for the maximum mass flow rate production of ammonia were determined using GA. These two reactor configurations were not compared under the same conditions. Penkuhn and Tsatsaronis (2016) used an advanced exergy analysis to compare two different systems for an ammonia synthesis loop. The results showed that the ammonia synthesis loop configuration using a three-staged AQCR has higher exergetic efficiency, and is superior from a thermodynamic point of view, compared to the IDCR.

Furthermore, in the literature reviewed by the authors of the present work, no study about the comparison between three types of ammonia synthesis fixed-bed reactor configurations in terms of cooling methods was found. In this work, firstly, a parametric sensitivity analysis is done based on a one-dimensional pseudo-homogeneous model to investigate the effect of various parameters on the N_2 conversion. Secondly, optimum operating conditions are found using differential evolution (DE) algorithm, as an efficient optimization technique, by considering the same catalyst volume, operating pressure and feed mass flow rate for all three types of reactor. Finally, a comparison between these three reactors configuration is carried out under the optimal operating conditions to response this question "which configuration is the best with regard to achieving the highest exit N_2 conversion at the lowest temperature profile along the reactor length".

2. Mathematical model

A one-dimensional pseudo-homogeneous model based on following assumptions was developed to determine the concentration and temperature distributions inside the reactors:

- The reactor operates at steady-state condition.
- The catalyst activity is uniform along the reactor and is considered equal to unity (assuming that the catalyst is new).
- Intra-particle mass and heat transfer restrictions are considered by a term that called effectiveness factor.
- The difference in temperature between the catalyst particle and the gas flowing past it has been evaluated by Kjaer (1958) and Eymery (1964) to be 2.3 °C at the top of the reactor (where the rate of reaction is a maximum), 0.6 °C near the middle and 0.4 °C at the outlet. These small temperature differences justify this assumption that the concentration and temperature of the gas flowing through the catalyst beds are equal to the catalyst particle.

- Axial dispersion of heat and mass is ignored in the light of results given by Eymery (1964). He showed that the inclusion of longitudinal dispersion term alters the steady-state temperature profile in the TVA reactor by less than 0.6 °C.

- Sadeghi and Kavianiboroujeni (2009) were shown that there is a good agreement between simulation results of the one/two-dimensional model and industrial data for ammonia synthesis AQCR; and the one and two-dimensional models behave closely to each other. This agreement justifies application of the one-dimensional model for optimization purposes to decrease the computational time. Therefore, in this study, the temperature and concentration gradients in the radial direction are neglected (one-dimensional model). This assumption is also confirmed by Kjaer (1958).
- The pressure drop along the reactor is negligible compared with the total pressure in the system in view of the results reported by Baddour et al. (1965).

To obtain the mass and energy balance equations, a differential element along the axial direction inside the reactor was considered.

2.1. Mass balance

The mass balance for IDCR, AQCR and AICR is expressed by:

$$\frac{dX_{N_2}}{dz} = \frac{\eta R_{NH_3} A}{2F^0_{N_2}} \tag{2}$$

2.2. Energy balance

The energy balance for the cooling tube and catalyst zone of IDCR, respectively, expressed by:

$$\frac{dT_f}{dz} = -\frac{\beta U A_i}{WC_{P_{mixf}}}\left(T_g - T_f\right) \tag{3}$$

$$\frac{dT_g}{dz} = -\frac{\beta U A_i}{WC_{P_{mixg}}}\left(T_g - T_f\right) - \frac{\Delta H_r \eta R_{NH_3} A}{WC_{P_{mixg}}} \tag{4}$$

$$\beta = \begin{cases} 1 \text{ for IDCR} \\ 0 \text{ for AQCR and AICR as a result of adiabatic performance} \end{cases} \tag{5}$$

where T_f and T_g are temperature of feed and reacting gas, respectively, and $C_{P_{mix}}$ is specific heat of the gas mixture. Shah (1967) developed equations for specific heat of pure components as a function of temperature and pressure as follows:

$$C_{pi} = A_i + B_i T + C_i T^2 + D_i T^3 \tag{6}$$

$$C_{p,NH_3} = 6.5846 - 0.61251 \times 10^{-2} T + 0.23663 \times 10^{-5} T^2 - 1.5981 \times 10^{-9} T^3 + [96.1678 - 0.067571P + (-0.2225 + 1.6847 \times 10^{-4} P)\, T + (1.289 \times 10^{-4} - 1.0095 \times 10^{-7} P)\, T^2] \tag{7}$$

where i represents H_2, N_2, CH_4, and Ar components; and A, B, C, and D are specific heat constants that is tabulated in Table 1.

Table 1 – Specific heat constants.

Component	A	$B \times 10^2$	$C \times 10^5$	$D \times 10^9$
H_2	6.952	−0.04576	0.09563	−0.2079
N_2	6.903	−0.03753	0.193	−0.6861
CH_4	4.750	1.2	0.303	−0.263
Ar	4.9675	0	0	0

2.3. Heat of reaction

Strelzoff (1981) developed a relation for calculation of heat of ammonia synthesis reaction as follows:

$$\Delta H_r = -\left[0.54526 + \frac{846.609}{T} + \frac{459.734 \times 10^6}{T^3}\right] P - 5.34685\, T - 0.2525 \times 10^{-3} T^2 + 1.69197 \times 10^{-6} T^3 - 9157.09 \tag{8}$$

2.4. Overall heat transfer coefficient

The overall heat transfer coefficient U by assumption of neglecting the thermal resistance of tubes wall is given by:

$$\frac{1}{U} = \frac{1}{h_{io}} + \frac{1}{h_o} \tag{9}$$

The following equation presented by De-wasch and Froment (1972) is used to calculate the heat transfer coefficient h_o inside the bed:

$$h_o = h_o^0 + \frac{0.0005924 Re'}{D_p} \tag{10}$$

The heat transfer coefficient h_{io} inside the cooling tubes is calculated according to the Colburn equation:

$$h_{io} = 0.0327 G\, C_{pmixf}\, (A_i/A_o)\, Re^{-0.2} \tag{11}$$

2.5. Rate of reaction

In order to estimate the rate of reaction, modified Timken equation was reported by Dyson and Simon (1968) is used as follows:

$$R_{NH_3} = 2k\left[K_a^2 a_{N_2}\left(\frac{a_{H_2}^3}{a_{NH_3}^2}\right)^{\alpha} - \left(\frac{a_{NH_3}^2}{a_{H_2}^3}\right)^{1-\alpha}\right] \tag{12}$$

where α is a constant between 0.5 and 0.75. In this work, $\alpha = 0.5$ is used.

K_a is equilibrium constant and the following relation proposed by Gillespie and Beattie (1930) is used to calculate it.

$$\log_{10} K_a = -2.691122 \log_{10} T - 5.519265 \times 10^{-5} T + 1.848863 \times 10^{-7} T^2 + \frac{2001.6}{T} + 26899 \tag{13}$$

k is the relation for reverse reaction of ammonia synthesis and calculated by Arrhenius equation (1979).

$$k = k_0 \exp\left(-\frac{E}{RT}\right) \tag{14}$$

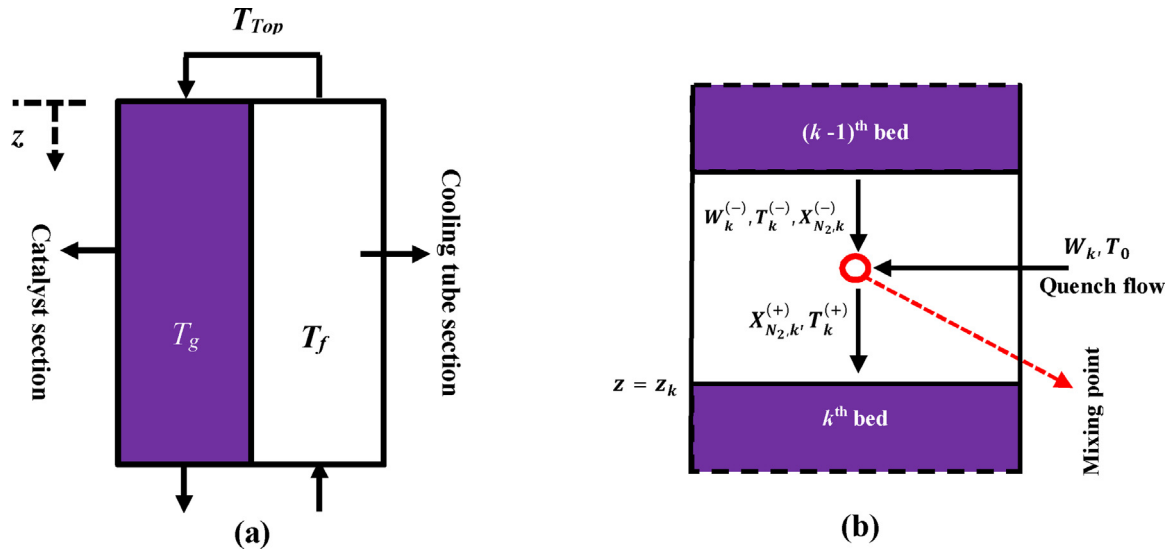

Fig. 2 – Lumped model for the (a) IDCR and (b) mixing point of gas stream and quench flow in the AQCR.

where k_0 is the Arrhenius coefficient, 8.849×10^{14}, and E is activation energy, 40,765 kcal/kmol.

The activity of a component is given by the following relation:

$$a_i = \frac{f_i}{f_i^0} \tag{15}$$

where f_i^0 is the reference fugacity and is assumed to be 1 atm. Hence:

$$a_i = \frac{f_i}{1} = f_i = y_i \phi_i P \tag{16}$$

where ϕ_i is the fugacity coefficient. Empirical relations for the fugacity coefficient of hydrogen, nitrogen and ammonia are determined by Dyson and Simon (1968) as follows:

$$\phi_{H_2} = \exp\left\{e^{\left(-3.8402T^{0.125}+0.541\right)}P - e^{\left(-0.1263T^{0.5}-15.98\right)}P^2 + 300\left[e^{(-0.011901T-5.941)}\left(e^{-\frac{P}{300}}-1\right)\right]\right\} \tag{17}$$

$$\phi_{N_2} = 0.93431737 + 0.3101804 \times 10^{-3}T + 0.295896 \times 10^{-3}P - 0.2707279 \times 10^{-6}T^2 + 0.4775207 \times 10^{-6}P^2 \tag{18}$$

$$\phi_{NH_3} = 0.1438996 + 0.2028538 \times 10^{-2}T - 0.4487672 \times 10^{-3}P - 0.1142945 \times 10^{-5}T^2 + 0.2761216 \times 10^{-6}P^2 \tag{19}$$

2.6. Effectiveness factor

In order to investigate the effect of resistance due to diffusion through the catalyst pores, an effectiveness factor (η) has been defined. Dyson and Simon (1968) developed an empirical relation for the effectiveness factor of particle size of 6–10 mm with respect to temperature and conversion as follows:

$$\eta = -4.6757259 + 0.02354872T + 4.687353X - 3.463308 \times 10^{-5} T^2 - 11.28031X^2 + 1.540881 \times 10^{-8}T^3 + 10.46627X^3 \tag{20}$$

2.7. Boundary conditions

The boundary conditions used to solve the model are discussed in this section.

2.7.1. IDCR

The IDCR can be lumped radially into two sections as shown in Fig. 2(a). At the top of the reactor where the gas reverses its direction to enter the catalyst section, the temperature is known and nitrogen is not converted to ammonia. Therefore, the boundary conditions are specified at the top of the reactor by:

$$\text{at } z = 0; \quad T_g = T_f = T_{Top}, \quad X_{N_2} = 0 \tag{21}$$

2.7.2. AQCR

A schematic diagram of lumped model for mixing point of gas stream and quench flow in the AQCR is shown in Fig. 2(b). The boundary condition used to solve the ordinary differential equations (ODEs) for the AQCR is:

$$\text{at } z = \begin{cases} 0 & T_g = T_1, \quad X_{N_2} = 0 \quad \text{for the first bed} \\ z_k & T_g = T_k^{(+)}, \quad X_{N_2} = X_{N_2,k}^{(+)} \quad \text{for the kth bed (k = 2, 3, …, N)} \end{cases} \tag{22}$$

where k is the number of each catalyst bed, and $X_{N_2,k}^{(+)}$ and $T_k^{(+)}$ are nitrogen conversion and temperature of mixture after the mixing point, respectively, that is calculated by the mass and energy balances around the mixing point as follows:

$$T_k^{(+)} = \frac{W_k^{(-)} C_{pk}^{(-)} T_k^{(-)} + W_k C_{p0} T_0}{C_{pk}^{(+)}\left(W_k^{(-)} + W_k\right)} \tag{23}$$

Table 2 – Strategy and parameters used for DE algorithm.

Parameter	Value
Population size (NP)	100
Scaling factor (F)	0.8
Crossover probability constant (CR)	0.1

$$X_{N_2,k}^{(+)} = \frac{W_k^{(-)} X_{N_2,k}^{(-)}}{W_k^{(-)} + W_k} \tag{24}$$

where $C_{pk}^{(-)}$, $T_k^{(-)}$ and $W_k^{(-)}$ are the specific heat, temperature and mass flow rate of gas coming from the previous catalyst bed, respectively, W_k is the mass flow rate of feed quenching to k^{th} catalyst bed, $X_{N_2,k}^{(-)}$ is nitrogen conversion before the mixing point, C_{p0} and T_0 are the specific heat and temperature of quench stream, and $C_{pk}^{(+)}$ is the specific heat of the gas mixture after the mixing point.

2.7.3. AICR

The boundary condition for the AICR as shown in Fig. 1(c) can be expressed as:

$$\text{at } z = z_k; \quad T_g = T_k, \quad X_{N_2} = X_{N_2,k} \tag{25}$$

where $X_{N_2,k}$ is the conversion of nitrogen output from $(k-1)^{th}$ catalyst bed.

2.8. Numerical method

In order to simultaneously solve the ODEs with the boundary conditions, the Runge–Kutta method of the forth order, with step size of 0.01 m, in the MATLAB programming environment is used.

3. Optimization

3.1. Differential evolution algorithm

In the last few years a differential evolution (DE) algorithm, which is fast and robust in numerical optimization, has been offered. DE algorithm is a stochastic optimization method minimizing an objective function that can model the problem's objectives while incorporating constraints. The algorithm essentially has three advantages; finding the true global minimum regardless of the initial parameter values, fast convergence, and using a few control parameters.

The basic strategy of DE algorithm can be found in literature (Storn and Price, 1997) and it consists of a four-step procedure: (1) choose randomly an initial population vector, (2) mutation, (3) crossover, and (4) selection. Different strategies can be adopted in DE algorithm based on the vector to be perturbed, number of difference vectors considered for perturbation, and finally the type of crossover used. Some general guidelines are available for choosing population size (NP), scaling factor (F), and crossover probability constant (CR). Details of the basic version of DE (pseudo code), its strategies, and choosing the parameters have been reported by Babu and Angira (2005, 2006), Babu and Munawar (2007), and Khademi et al. (2009, 2010, 2011). In this optimization problem, the DE/best/1/bin strategy is applied and parameters used for DE algorithm are reported in Table 2.

3.2. Optimization problem formulation

In this study, maximization of the objective namely, nitrogen conversion at the reactor outlet is considered. The objective is as follows:

$$J = X_{N_2} \tag{26}$$

In order to prevent catalyst sintering, the temperature must be lower than 800 K along the reactor. Therefore, the following constraint is considered.

$$T_g < 80\,K \tag{27}$$

This constraint should be regarded in the optimization process. The penalty function method has been used to incorporate this constraint into the objective function (Eq. (26)). In this method, a penalty parameter is defined in a way to eliminate the unacceptable results automatically. The penalty function takes a finite value when a constraint is violated and a value of zero when constraint is satisfied. In this work, the value of penalty parameter is considered 10^7, but this value depends on the order of magnitude of the decision variables in the problem. Finally, the objective function regarded for minimization is:

$$OF = -J + 10^7 G^2 \tag{28}$$

where

$$G = \max\left\{0, (T - 800)\right\} \tag{29}$$

The optimization problem is solved using the proposed algorithm, DE.

To compare these three types of reactor in terms of applied cooling methods, the pressure and total mass flow rate of feed gas are assumed constant and not considered as decision variables. The picked decision variables are different for each reactor as follows:

3.2.1. IDCR

One decision variable namely, temperature of feed gas at the top of the reactor (top temperature), T_{Top}, is considered for optimization of IDCR. The range of top temperature is:

$$666 < T_{Top} < 726\,K \tag{30}$$

The reason for choosing this range of top temperature is explained in the Section 4.3.1.

3.2.2. AQCR

The temperature of feed gas to the first bed, T_1, dimensionless length of each bed, ξ_k, and fraction of total feed flow rate quenching to each bed, f_{W_k}, are considered as decision variables for optimization of AQCR; where k is the number of each catalyst bed. The dimensionless length of bed is defined as the fraction of total bed length. While the nitrogen conversion is directly dependent on the bed length and flow rate of quenched stream, these parameters are selected as decision variables. The ranges of these decision variables are:

$$623 < T_1 < 773\,K \tag{31}$$

$$0 < \xi_k < 1 \tag{32}$$

$$0 < f_{W_k} < 1 \tag{33}$$

To ensure that the temperature of synthesis gas at the inlet of the first bed is not too low for the ammonia synthesis reaction to occur, the lower bound on inlet temperature set at 623 K. At high temperatures, catalyst starts to deactivate; for this reason an upper bound of 773 K is chosen for inlet gas temperature.

The total feed flow rate, W, should be distributed between the reactor beds (see Fig. 1(b)). Also, the total volume of catalyst should be divided to all the beds. Therefore, for optimization of AQCR, two equality constraints are integrated with the inequality constraint as follows:

$$\sum_{k=1}^{N} \xi_k = 1 \tag{34}$$

$$\sum_{k=1}^{N} f_{W_k} = 1 \tag{35}$$

It should be noted, since hydrogen and nitrogen come from the previous unit, the temperature of quench streams, T_0, is assumed constant.

3.2.3. AICR

The temperature of inlet gas to each bed, T_k, and dimensionless length of each bed, ξ_k are selected as decision variables. These variables ranges considered in this study are:

$$623 < T_k < 773\,K \tag{36}$$

$$0 < \xi_k < 1 \tag{37}$$

The reason to choose these domains is mentioned in the previous section. Also, Eq. (34) is considered as an equality constraint to optimize the AICR.

4. Results and discussion

4.1. Base case

In order to establish a reference point, simulation is carried out for a "base case". The IDCR design data and operating conditions for the base case are reported in Table 3. The geometry and operating conditions are similar to those used by Murase et al. (1970).

In order to compare the results of optimization in the same conditions, the feed mass flow rate, operating pressure and catalyst volume for all three types of reactor are considered to be the same. In other words, the weight hourly space velocity (WHSV) is assumed to be constant. The geometry and operating conditions of the AQCR and AICR, for the base case, are tabulated in Table 4.

4.2. Simulation results and model validation

The calculated temperature profiles of feed and reacting gas as well as the variation of ammonia mole fraction for the IDCR are shown in Fig. 3. As it can be seen in this figure, the feed gas is heated inside the tubes from 515 K to 694 K (top temperature) along the reactor length. At the entrance of catalyst zone, reacting gas temperature increases smoothly and a hot spot develops and then decreases to 735 K. Before a certain position along the catalyst zone (dimensionless length = 0.5), the generated heat flux is higher than the transferred heat from the solid wall, the system starts to heat up and the highest temperature, 800 K, is observed at this position. Afterward, the generated heat flux decreases, mainly due to fuel depletion. The opposite situation occurs and the system starts to cool down.

Fig. 3 indicates the ammonia mole fraction increases rapidly; most of the reaction occurring in the top half of the catalyst bed where the rate of the reaction is high; then the conversion is brought under control as a result of the depressing effect of the decreasing nitrogen concentration on the reaction rate.

Also in Fig. 3, the mathematical model of IDCR is validated against the actual plant data provided by Allgood (Baddour et al., 1965; Murase et al., 1970) under the design specifications and input data listed in Table 3. The calculated value of the ammonia mole fraction at the reactor exit is 0.2022, which

Table 3 – Operating conditions and design data of the IDCR that is reported by Murase et al. (1970).

Parameter	Value
Operating conditions	
Pressure	286 atm
Top temperature	694 K
Feed mass flow rate	26400 kg/h
Feed composition	
y_{NH_3}	0.05
y_{N_2}	0.6525
y_{H_2}	0.2175
y_{Ar}	0.04
y_{CH_4}	0.04
Catalyst zone	
Reactor length	5.18 m
Total volume of catalyst bed	4.07 m^3
Reactor basket diameter	1.1 m
Reactor basket cross-section area	0.95 m^2
Catalyst zone cross-section area	0.78 m^2
Cooling tube	
Surface area of cooling tubes per unit length of reactor	10 m^2/m
Number of tubes	84
Tube outside diameter	50.8 mm
Tube inside diameter	38.1 mm
Tube heat exchanger area (outer)	69.4 m^2
Tube heat exchanger area (inner)	52 m^2

Table 4 – Geometry and operating conditions of the AQCR and AICR.

Parameter	Value
Operating conditions	
Pressure	286 atm
Feed mass flow rate	26,400 kg/h
Quench flow temperature	600 K
Fraction of total feed flow rate quenching to each bed	0.5
Feed temperature to the first bed of AQCR	700 K
Inlet gas temperature to the first bed of AICR	720 K
Inlet gas temperature to the second bed of AICR	680 K
Geometry conditions	
Number of catalyst bed	2
Dimensionless length of each bed	0.5
Total volume of catalyst bed	4.07 m^3
Reactor basket diameter	1.1 m

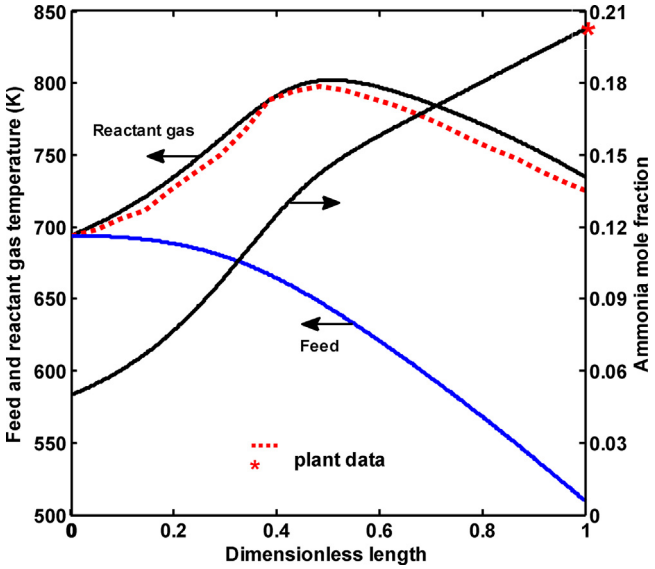

Fig. 3 – Variation of the feed and reactant gas temperature as well as ammonia mole fraction along the IDCR.

is in acceptable agreement with the plant data, 0.200728. At the reactor outlet, the reacting gas temperature obtained from the model is 12 °C higher than the plant outlet temperature; the hot spot for the model is 0.3 m lower and the maximum temperature is 4 °C higher than that in the plant reactor. No actual plant data are available for comparison with the feed temperature in the cooling tubes. Thus, the simulation data are in fairly good agreement with the plant data and the proposed model is an acceptable approximation of the actual plant; this model also will be reliable for simulation and optimization of the AQCR and AICR.

4.3. *Sensitivity analysis*

A parametric sensitivity analysis is carried out to assess the impact of various parameters, one at a time, on the nitrogen conversion. The simultaneous effect of inlet and top temperature on the stability of IDCR is investigated. In this regard, the AQCR is simplified to two catalyst beds with one quench flow to study the influence of the dimensionless length of the first bed and the fraction of feed flow rate quenching to the 2nd bed as well as the temperature of inlet gas to the first bed on N_2 conversion. Finally, the sensitivity of N_2 conversion to dimensionless length of each bed and the inlet gas temperature to the 2nd bed is investigated for the AICR with two catalyst beds.

4.3.1. *IDCR*

The stability of the reactor can be expressed in terms of change of the top temperature corresponding to the inlet temperature. The S-shaped curve of the top temperature versus inlet gas temperature to the cooling tubes of the IDCR is reperesented in Fig. 4; as each point on this curve illustrates a solution to the conservation equations in the catalyst zone. Point E (493 K) known as the blow-out temperature is the minimum temperature in the cooling tubes, below which stable operation of the reactor is not possible and no chemical reaction occurs. Therefore, for the temperatures less than 493 K, the inlet temperature to the cooling tubes is equal to the top temperature. The curve also indicates another point D (545 K), the ignition point, above which causes sintering of the catalyst. In the region between points E and D, for each inlet temperature to the cooling tubes there are three top temperatures, an example of which is shown by the dashed line. Thus, the IDCR can have three physically real points, A, B and C, at which the boundary conditions relating to the system are satisfied. At the stable point C, significant reaction does not take place because the feed is too cold. The extent of the reaction is greatest at the stable point A and this is the operating steady state. At the intermediate point B, a small perturbation would result in either reactor blow-out or heat-up; so this point is unstable. Thus in Fig. 4 only the branch of the curve to the above of the point E is stable operation of the IDCR. Consequently, to optimize the reactor, the temperature 666 and 726 K are chosen as the lower and upper bounds of top temperature (Eq. (26)) corresponding to this stable branch of curve and points D and E. Upreti and Deb (1997) reported that top temperature lower than 666 K leads to begin the reverse reaction. This statement confirms the results of this research.

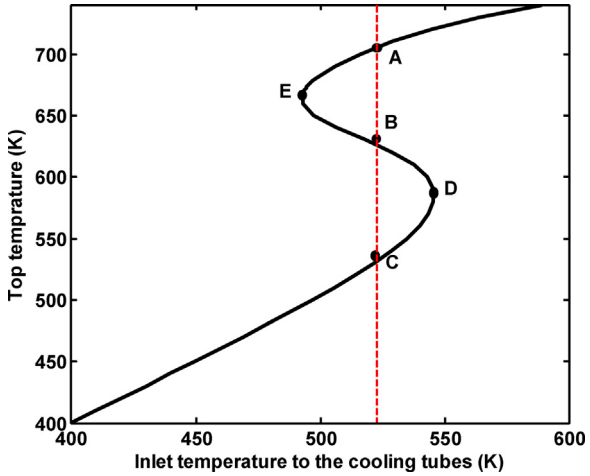

Fig. 4 – Variation of the top temperature versus the inlet gas temperature to the cooling tubes of the IDCR.

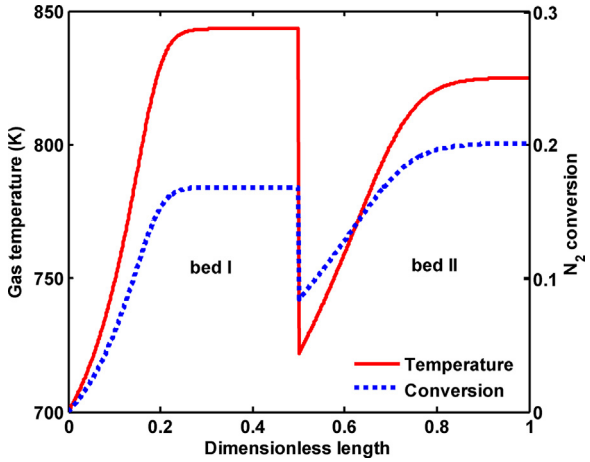

Fig. 5 – N_2 conversion and temperature profile along the 2-bed AQCR.

4.3.2. *AQCR*

Fig. 5 illustrates the N_2 conversion and temperature profiles along the 2-bed AQCR, at the base case. Simulation results show that the reactor conditions vary within the two beds. The discontinuity occurring in the profiles are due to the injection of the quench flow between two beds. The quench flow decreases the conversion between the first and second bed however; it will develop along the second bed. The slope of N_2

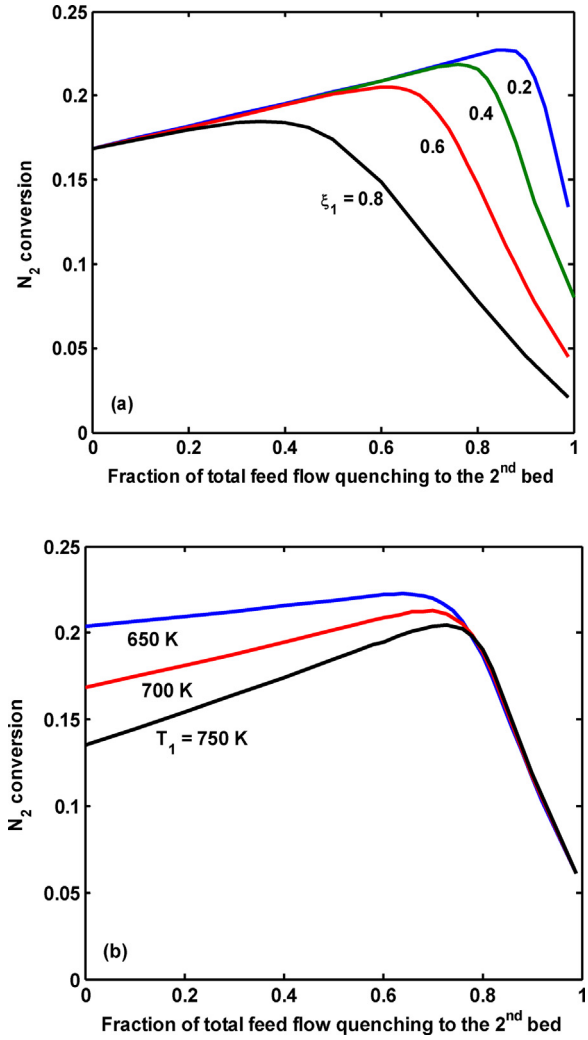

Fig. 6 – Effect of the fraction of feed flow rate quenching to the 2nd bed on the N_2 conversion at various (a) dimensionless lengths of the first bed, and (b) inlet gas temperatures to the first bed.

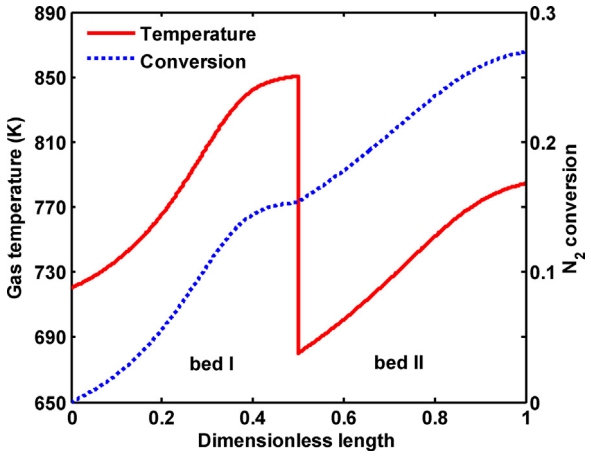

Fig. 7 – N_2 conversion and temperature profiles along the 2-bed AICR.

conversion profile in the first bed is more than that in the second bed. This trend says that ammonia production decreases from first to second bed. Similar trend occurs for temperature profile along the reactor. As a result of exothermicity of the reaction and adiabaticity of the reactor, the temperature rises along each bed. As seen in Fig. 5, the conversion and temperature profiles remain unchanged in the range of 0.2–0.5 and 0.8–1, which shows ammonia synthesis reaction reaches to equilibrium state in these regions and so, part of the catalyst bed is useless. Consequently, the feed temperature and dimensionless length of each bed must be optimized.

The effect of various parameters on the maximum N_2 conversion at the reactor exit is studied from the relation between the fraction of feed flow rate quenching to the 2nd bed and the N_2 conversion at the reactor exit. The effect of the dimensionless length of the first bed and the inlet gas temperature to the first bed is indicated, respectively, in Fig. 6(a) and (b). As it can be seen in Fig. 6(a), the conversion increases smoothly with the fraction of feed flow rate quenching to the 2nd bed and a maximum point develops, and then decreases rapidly. An increase in the fraction of feed flow quenching to the 2nd bed leads to a decrease in the inlet gas temperature to the second bed. Whereas the ammonia synthesis is a reversible exothermic reaction, by reduction of gas temperature, the system will modify to neutralize the effect of this change. The equilibrium shifts to the right, based on Le Chetalier's principle, and results in increasing the conversion to reach a maximum point. After that, the conversion at the reactor outlet decreases as a result of exiting a part of gas from the reactor in the form of unreacted. Decreasing the dimensionless length of the first bed causes the migration of the maximum point toward the right, as well as an increase in the conversion at this maximum point (see Fig. 6(a)). Therefore, by increasing the length of second bed and fraction of total feed flow quenching to 2nd bed, the maximum conversion increases.

In Fig. 6(b), the inlet gas temperature to the first bed does not significantly influence the location of the maximum point, but the magnitude of the maximum conversion increases. A decrease in the inlet gas temperature to the first bed leads to a decrease in the gas temperature along the reactor length; consequently, the conversion increases.

4.3.3. AICR

The variation of N_2 conversion and gas temperature along the 2-bed AICR are indicated in Fig. 7, at the base case. The conversion increases along the length of the reactor. In the middle of the reactor, the temperature at once falls from 850 to 680 K as a result of cooling between two catalyst beds by an external heat exchanger. As seen in this figure, the gas temperature is above 800 K in the range of 0.3–0.5 (dimensionless length), which as mentioned above to prevent catalyst sintering, the temperature must be lower than 800 K along the reactor. Thus, the operating parameters should be changed in a manner to operate the reactor under optimum conditions.

The influence of the inlet gas temperature to the second bed on the maximum N_2 conversion at the reactor exit is investigated from the relevance between the dimensionless length of the first bed and the N_2 conversion at the reactor exit, as shown in Fig. 8. Increasing the dimensionless length of the first bed (ξ_1) results in increasing the gas residence time in the first bed and decreasing the gas temperature along the second bed length, which both are in the direction of increasing ammonia production; thus, initially the conversion increases. After maximum point, the conversion reduces with the dimensionless length of the first bed because of two reasons: (1) the gas residence time in the second bed decreases, (2) reaction reaches to the equilibrium state along the end part of the first catalyst bed, therefore, this part remains unused at the constant feed flow rate. Increasing the inlet gas temperature to the second bed leads to migration of the location of maximum

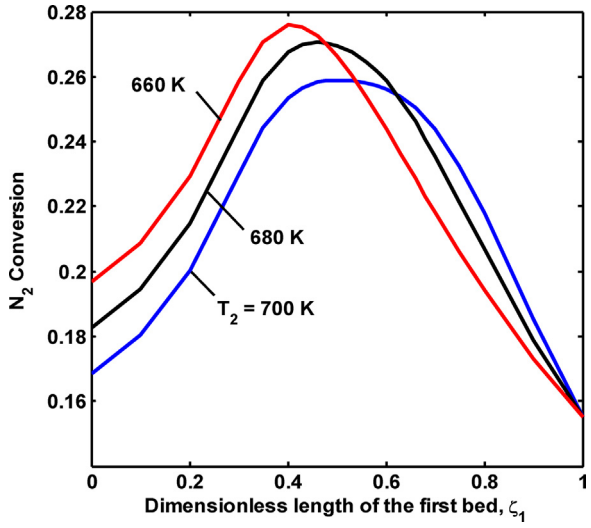

Fig. 8 – Effect of the dimensionless length of the first bed on the N_2 conversion at various inlet gas temperatures to the second bed.

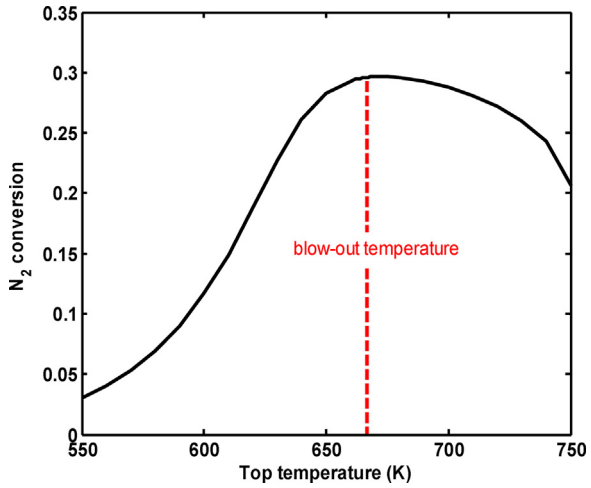

Fig. 9 – Changes of the N_2 conversion at the IDCR exit versus the top temperature.

point toward the right, as well as a decrease in the exit conversion at this maximum point. Similarly, the effect of inlet gas temperature to the first bed on the maximum N_2 conversion at the reactor outlet is similar to the trend observed in Fig. 8.

4.4. *Optimization results*

With due attention to the parametric sensitivity analysis carried out in section 4.3; various parameters for each reactor are selected as decision variables to maximize the nitrogen conversion subject to constraints. In order to optimize the reactors, the DE code is coupled with the non-linear mathematical model (Eqs. (2)–(16)) and the following results have been obtained.

4.4.1. *IDCR*

The variation of N_2 conversion at the reactor exit versus the top temperature is shown in Fig. 9. The ammonia synthesis is a reversible exothermic reaction, thus the relation between the N_2 conversion at the reactor exit and the reaction temperature shows a maximum point (see Fig. 9). Before this maximum point, the conversion is affected by the low reaction rate due to the low temperature; after this point, the conversion is influenced by the equilibrium yield, which decreases with temperature. Therefore, this figure reveals the existence of an optimum top temperature equal to 673 K for the IDCR. At this optimal condition, the inlet gas temperature to the cooling tubes is 495 K. The results indicate that the maximum conversion at the reactor exit, 0.3, is obtained near the blow-out temperature, 666 K.

Table 5 – Optimized decision variables for the 2, 3 and 4-bed AQCR.

Parameter	Value		
	2-bed	3-bed	4-bed
ξ_1	0.31	0.13	0.08
ξ_2	0.69	0.25	0.08
ξ_3	–	0.62	0.24
ξ_4	–	–	0.60
f_{w_1}	0.39	0.20	0.14
f_{w_2}	0.61	0.26	0.10
f_{w_3}	–	0.54	0.24
f_{w_4}	–	–	0.52
T_1 (K)	625	635	644
X_{N_2}	0.24	0.26	0.26
Exit gas temperature (K)	800	792	792

Table 6 – Optimized decision variables for the 2, 3 and 4-bed AICR.

Parameter	Value		
	2-bed	3-bed	4-bed
ξ_1	0.50	0.33	0.25
ξ_2	0.50	0.33	0.25
ξ_3	–	0.33	0.25
ξ_4	–	–	0.25
T_1 (K)	660	696	714
T_2 (K)	672	696	696
T_3 (K)	–	697	711
T_4 (K)	–	–	708
X_{N_2}	0.27	0.30	0.30
Exit gas temperature (K)	773	757	752

4.4.2. *AQCR*

The optimal conditions for the 2, 3 and 4-bed AQCR to preventing hotspots and keeping the reactor thermally stable are summarized in Table 5. It can be seen from the optimization results that the optimum catalyst bed lengths increase from first to last, for example, for 3-beds AQCR, the optimal dimensionless lengths increase from the first bed (0.13) to the last one (0.62). This leads to conversion value close to the equilibrium one at the bed outlet. This trend also occurs for the optimal fraction of total feed flow rate quenching to each bed, which nearly increases from first to last.

As observed from Table 5, the 3-bed AQCR is the most efficient reactor in terms of ammonia production, saving energy, and capital and maintenance costs, which can be concluded from the following: (1) The conversion in 3 and 4-bed reactor is higher than that in 2-beds (0.26 in comparison with 0.24); (2) The temperature of feed gas to the first bed in 3-beds reactor is lower than that in 4-beds which leads to saving energy in the preheater; (3) The capital and maintenance costs for 4-beds reactor is more than that for 3-beds.

4.4.3. *AICR*

Table 6 presents the optimal geometry and operating conditions for the 2, 3 and 4-bed AICR. The interesting point is that

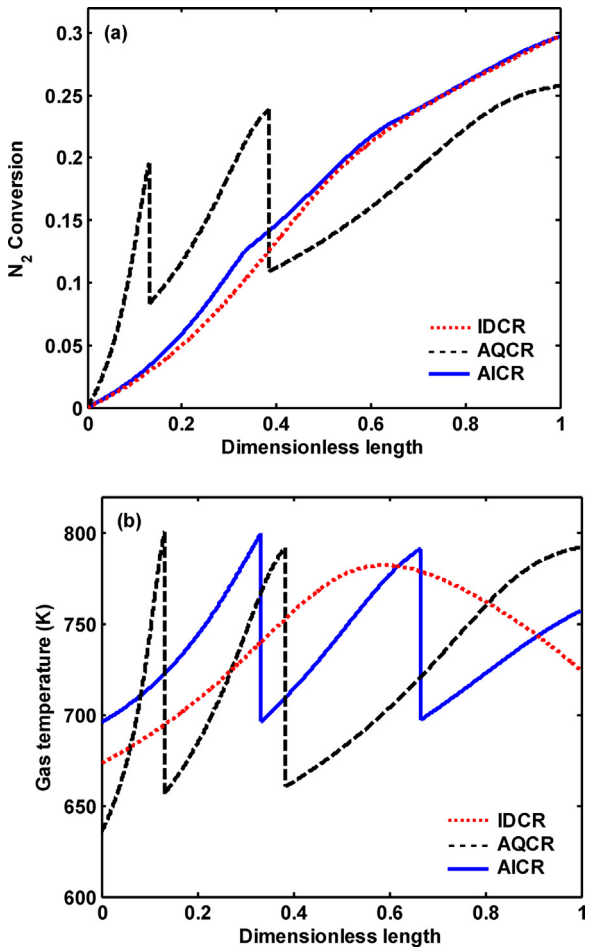

Fig. 10 – A comparison between the IDCR, 3-bed AQCR and 3-bed AICR under optimal conditions in terms of (a) N_2 conversion, and (b) temperature profiles.

the length of the beds is the same in optimal conditions, e.g., in 3-beds AICR, the length of each bed is 0.33. Since the exit gas temperature from 3 and 4-bed reactors is almost 20 K less than that from 2-beds; and the conversion in 3 and 4-beds reactors is more than that in 2-beds (0.3 in comparison with 0.27), so, the 3 and 4-bed reactors are more efficient than 2-beds reactor. In accordance with the optimum inlet gas temperature to each bed, a set of heat exchangers should be designed with different sizes or cooling mediums between each bed. Due to the increasing of capital cost and number of heat exchangers with the number of beds, therefore, the 3-bed reactor is the best one between these three AICR.

4.4.4. *Comparison between three types of reactor*

A comparison between the IDCR, 3-bed AQCR and 3-bed AICR under optimal conditions in terms of N_2 conversion and gas temperature along the reactor is presented in Fig. 10(a) and (b). While the first bed of the AQCR has the smallest length, it is responsible for most of the variations in conversion. In contrast, little change in the conversion is due to the third bed which has the highest length. It can be seen that the N_2 conversion (also gas temperature) improves with the dimensionless length of each bed in 3-bed AQCR, but the increase of the rate decreases gradually. This is because the mixture of reacting gas and raw material gas results in changes in proportion of the reactant and product gases, lowering the conversion and reaction temperature. The IDCR and AICR have a similar behavior in terms of N_2 conversion. In both of them, the conversion profiles are close to each other and rise along the reactor length until they reach to 0.3 at the reactor exit. Almost the first half of the reactor (dimensionless length = 0–0.4), although the conversion in the AQCR is more than two other reactors, however after this position along the reactor, the conversion in AQCR becomes lower than that in the two other reactors and approaches to 0.26 at the reactor exit. The comparison of N_2 conversion in AQCR with IDCR and AICR shows that the conversion at the output of AQCR is decreased by 13.3%. So, the AQCR is the least significant type of reactor in terms of ammonia production. Although the reactants are fed to the AQCR at the low temperature 635 K (see Fig. 10(b)), but the temperature reaches to 800 K at the end of the first bed and products are removed from the reactor at the high temperature 792 K which results in wasting a lot of energy in the reactor. It is noteworthy that the AQCR has an advantage over the AICR in terms of temperature easy control and not using cooling devices such as external heat exchanger between each bed.

The comparison between temperature profiles in IDCR and AICR indicates that the feed gas temperatures are 490 and 696 K, and the exit gas temperatures are 725 and 757 K, respectively. Therefore, the IDCR operates at a lower temperature level respect to the AICR, which leads to saving energy and increasing the life of the catalyst and the reactor material. The other benefit of IDCR over AICR is that you do not need the cooling medium to remove the heat from the reactor. In general, from the standpoint of cooling methods to achieve the most ammonia production, the IDCR, AICR and AQCR are various ammonia synthesis reactor configurations from the most desirable to the least desirable.

5. Conclusions

In the present study, a one-dimensional pseudo-homogeneous model was applied for simulation of ammonia synthesis reactor in three types: internal direct cooling reactor, adiabatic quench cooling reactor and adiabatic indirect cooling reactor. A set of ODEs was solved by the Runge–Kutta method of the forth order and the model was validated against the actual plant data provided by Allgood (Baddour et al., 1965; Murase et al., 1970). A parametric sensitivity analysis was carried out to assess the impact of various parameters on the nitrogen conversion at the outlet of IDCR, 2-bed AQCR and 2-bed AICR. Differential evolution (DE) algorithm was employed to optimize ammonia synthesis process in IDCR, 2/3/4-bed AQCR and 2/3/4-bed AICR. In this regard, maximum N_2 conversion was defined as the objective function to determine the optimal operating conditions. The feed mass flow rate, operating pressure and catalyst weight for all three types of reactor were considered to be the same and not selected as decision variables. Finally, a comparison between these reactor configurations was carried out under the optimal operating conditions and the following key results are achieved:

- In the 2-bed AQCR, the maximum value of the conversion at the reactor exit can be increased by decreasing the dimensionless length of the first bed, and also by reducing the inlet temperature to the first bed.
- The behavior of the conversion at the outlet of 2-bed AQCR with the fraction of feed flow rate quenching to the 2nd bed is similar to the behavior of the conversion at the outlet of

2-bed AICR with the dimensionless length of the first bed. In both of them, the conversion increases; a maximum point develops, and then decreases rapidly.

- Since the optimum top temperature in IDCR (673 K) is near the blow-out temperature (666 K), so the gas temperature to the cooling tube must be controlled to 495 K in order to achieve a maximum N_2 conversion of 0.3.
- The 3-bed AQCR is the most efficient reactor in comparison with 2 and 4-beds in terms of ammonia production, saving energy, and capital and maintenance costs; in which the temperature of feed gas to the first bed, 635 K, dimensionless length of each bed, 0.13, 0.25 and 0.62, and fraction of total feed flow rate quenching from the first to end bed, 0.2, 0.26 and 0.54 are the optimal operating conditions to get a maximum conversion of 0.26.
- A comparison between 2, 3 and 4-beds AICR shows a superior efficiency of 3-beds reactor in terms of the highest conversion and the lowest number of external heat exchanger between each bed. The optimum value of N_2 conversion is found 0.3 in 3-bed AICR at inlet gas temperature to each bed, 696 K, and dimensionless length of each bed, 0.33.
- Under the optimal operating conditions, the conversion profiles in the IDCR and AICR are close to each other, but they have not a similar behavior in terms of temperature profile.
- The most important result of this study: IDCR, 3-bed AICR and 3-bed AQCR are from the most favorable to the least favorable configuration for ammonia synthesis process. Therefore, the most efficient cooling method is the IDCR.

References

Azarhoosh, M.J., Farivar, F., Ale Ebrahim, H., 2014. Simulation and optimization of a horizontal ammonia synthesis reactor using genetic algorithm. R. Soc. Chem. 4, 13419–13429.

Babu, B.V., Angira, R., 2005. Optimal design of an auto-thermal ammonia synthesis reactor. Comput. Chem. Eng. 29, 1041–1045.

Babu, B.V., Angira, R., 2006. Modified differential evolution (MDE) for optimization of non-linear chemical processes. Comput. Chem. Eng. 30, 989–1002.

Babu, B.V., Angira, R., Nilekar, A., 2004. Optimal design of an auto-thermal ammonia synthesis reactor using differential evolution. In: Proceedings of The Eighth World Multi-Conference on Systematics, Cybernetics and Informatics (SCI-2004), Orlando, Florida, USA, July 18–21, pp. 132–137.

Babu, B.V., Munawar, S.A., 2007. Differential evolution strategies for optimal design of shell- and-tube heat exchangers. Chem. Eng. Sci. 62, 3720–3739.

Baddour, R.F., Brian, P.L.T., Logeais, B.A., Eymery, J.P., 1965. Steady-state simulation of an ammonia synthesis converter. Chem. Eng. Sci. 20, 281–292.

Borges, R.A., Lobato, F.S., Steffen-Jr, V., 2012. Modeling and optimization of an auto-thermal ammonia synthesis reactor using the gravitational search algorithm. In: 3rd International Conference on Engineering Optimization, Rio de Janeiro, Brazil, July 01–05.

Carvalho, E.P., Borges, C., Andrade, D., Yuan, J.Y., Ravagnani, M.A.S.S., 2014. Modeling and optimization of an ammonia reactor using a penalty-like method. Appl. Math. Comput. 237, 330–339.

Dashti, A., Khorsand, K., Ahmadi Marvast, M., Kakavand, M., 2006. Modeling and simulation of ammonia synthesis reactor. Pet. Coal 48, 15–23.

De-wasch, A.P., Froment, G.F., 1972. Heat transfer in packed beds. Chem. Eng. Sci. 27, 567–576.

Dyson, D.C., Simon, J.M., 1968. A kinetic expression whit diffusion correction for ammonia synthesis on industrial catalyst. Ind. Eng. Chem. Fundamen. 7, 605–610.

Elnashaie, S.S., Abashar, M.E., Al-Ubaid, A.S., 1988a. Simulation and optimization of an industrial ammonia reactor. Ind. Eng. Chem. Res. 27, 2015–2022.

Elnashaie, S.S.E.H., Mahfouz, A.T., Elshishini, S.S., 1988b. Digital simulation of an industrial ammonia reactor. Chem. Eng. Process. 23, 165–177.

Eymery, J.P., 1964. The Dynamic Behavior of an Ammonia Synthesis Reactor. D.Sc. Thesis. M.I.T.

Gaines, L.D., 1977. Optimal temperatures for ammonia synthesis converters. Ind. Eng. Chem. Process Des. Dev. 16, 381–389.

Gillespie, L.J., Beattie, J.A., 1930. The thermodynamic treatment of chemical equilibria in systems composed of real gases. I. An approximate equation for the mass action function applied to the existing data on the haber equilibrium. Phys. Rev. 36, 743.

Khademi, M.H., Farsi, M., Rahimpour, M.R., Jahanmiri, A., 2011. DME synthesis and cyclohexane dehydrogenation reaction in an optimized thermally coupled reactor. Chem. Eng. Process. 50, 113–123.

Khademi, M.H., Rahimpour, M.R., Jahanmiri, A., 2010. Differential evolution (DE) strategy for optimization of hydrogen production, cyclohexane dehydrogenation and methanol synthesis in a hydrogen-permselective membrane thermally coupled reactor. Int. J. Hydrogen Energy 35, 1936–1950.

Khademi, M.H., Setoodeh, P., Rahimpour, M.R., Jahanmiri, A., 2009. Optimization of methanol synthesis and cyclohexane dehydrogenation in a thermally coupled reactor using differential evolution (DE) method. Int. J. Hydrogen Energy 34, 6930–6944.

Kjaer, J., 1958. Measurements and Calculation of Temperature and Conversion in Fixed-Bed Catalytic Reactors. Jui. Gjellerups Forlag, Copenhagen.

Ksasy, M.S.M., Areed, F., Saraya, S., Khalik, M.A., 2010. Optimal reactor length of an auto-thermal ammonia synthesis reactor. Int. J. Electr. Comput. Sci. 10, 6–15.

Murase, A., Roberts, H.L., Converse, A.O., 1970. Optimal thermal design of an auto-thermal ammonia synthesis reactor. Ind. Eng. Chem. Process Des. Dev. 9, 503–513.

Penkuhn, M., Tsatsaronis, G., 2016. Comparison of different ammonia synthesis loop configurations with the aid of advanced exergy analysis. In: The 29th International Conference on Efficiency, Cost, Optimization, Simulation and Environmental Impact of Energy Systems, June 19–23, Portoroz, Slovenia.

Reddy, K.V., Husain, A., 1982. Modeling and simulation of an ammonia synthesis loop. Ind. Eng. Chem. Process Des. Dev. 21, 359–366.

Sadeghi, M.T., Kavianiboroujeni, A., 2009. The optimization of an ammonia synthesis reactor using genetic algorithm. Int. J. Chem. Reactor Eng. 6, 1–18.

Shah, M.J., 1967. Control simulation in ammonia production. Ind. Eng. Chem. 59, 72–83.

Storn, R., Price, K., 1997. Differential evolution — a simple and efficient heuristic for global optimization over continuous spaces. J. Global Optim. 11, 341–359.

Strelzoff, S., 1981. Technology and Manufacture of Ammonia. Wiley, New York.

Upreti, S.R., Deb, K., 1997. Optimal design of an ammonia synthesis reactor using genetic algorithms. Comput. Chem. Eng. 21, 87–92.